

**A Facile Visualized Solid-Phase Detection of Virus-Specific Nucleic Acid
Sequences through an Upconversion Activated Linear Luminescence Recovery**

Process

Xiaorong Liu^{a,1}, Chaonan He^{b,1}, Qi Huang^a, Mengmeng Yu^c, Zhuang Qiu^c, Haoxin Cheng^a, Yifei Yang^c, Xian Hao^{c*}, and Xiaolei Wang^{a, b*}

a. College of Chemistry, Nanchang University, Nanchang, Jiangxi, 330088 (P.R. China)

b. The National Engineering Research Center for Bioengineering Drugs and the Technologies, Institute of Translational Medicine, Nanchang University, Nanchang, Jiangxi, 330088 (P.R. China)

c. School of Public Health & Jiangxi Provincial Key Laboratory of Preventive Medicine, Nanchang, Jiangxi, 330088 (P.R. China)

* Corresponding authors: xian.hao@ncu.edu.cn, wangxiaolei@ncu.edu.cn

1 These authors contributed equally to this work.

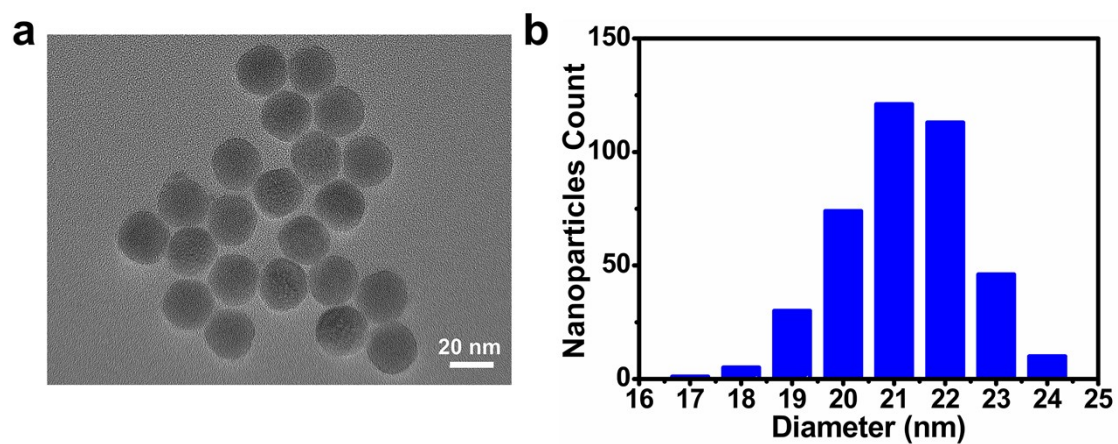


Figure S1. (a) TEM image of OA-capped NaYF₄:Yb, Er core UCNPs. (b) Histogram of particle size for core UCNPs (the data was obtained from the TEM images over more than 400 core UCNPs).

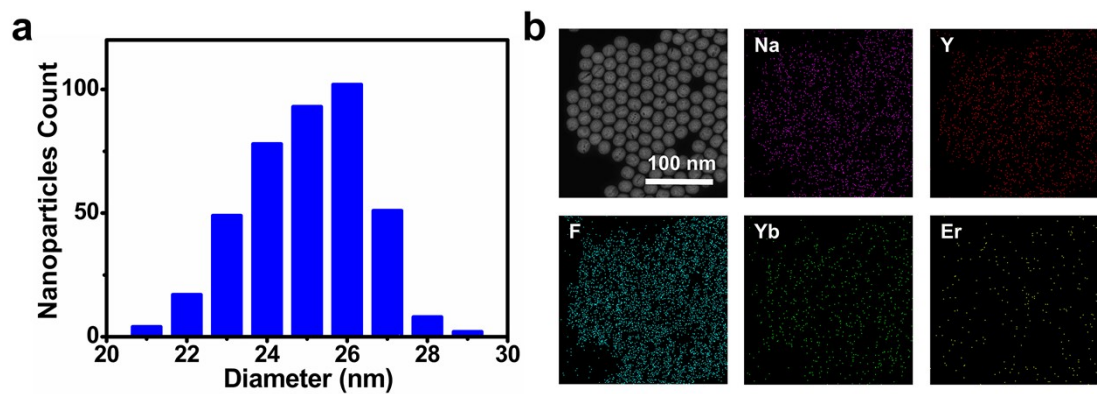


Figure S2. (a) Histogram of particle size for core/shell UCNPs (the data was obtained from the TEM images over more than 400 core/shell UCNPs). (b) TEM and the elemental mapping images for Na, Y, F, Yb and Er of NaYF₄:Yb, Er@NaYF₄ core/shell UCNPs.

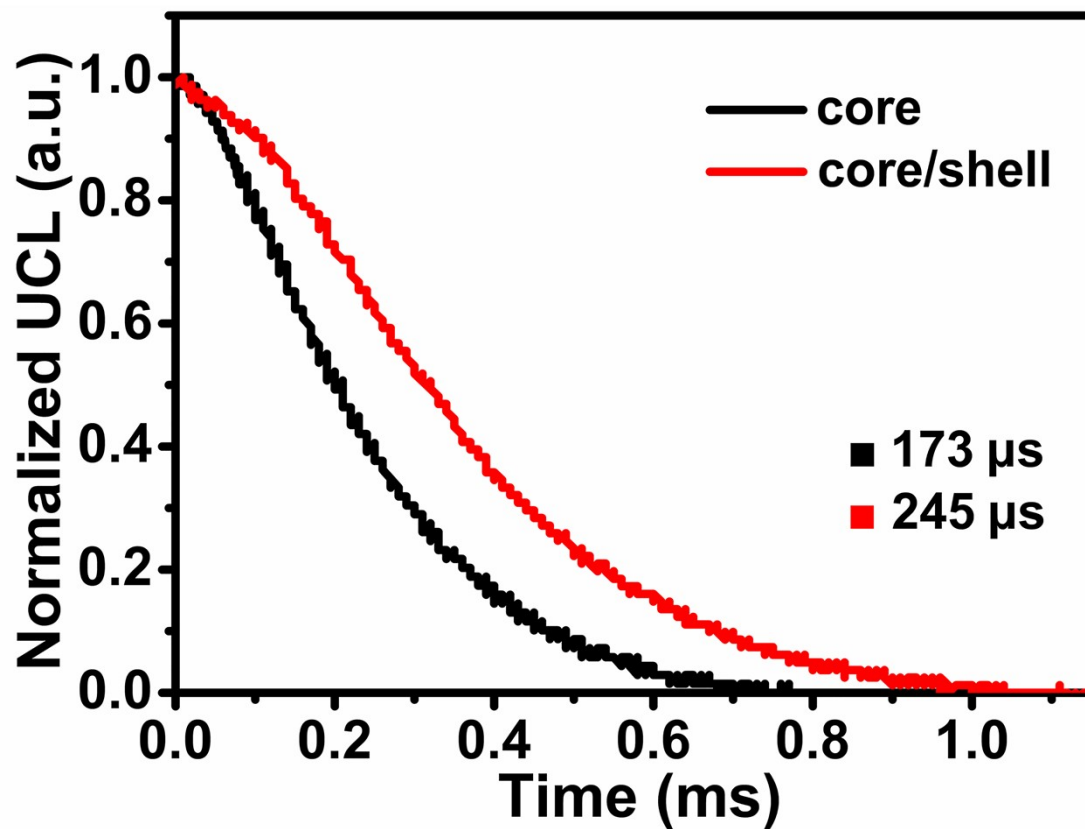


Figure S3. UCL lifetime curves at 541 nm for the core and core/shell UCNPs under 980 nm laser irradiation.

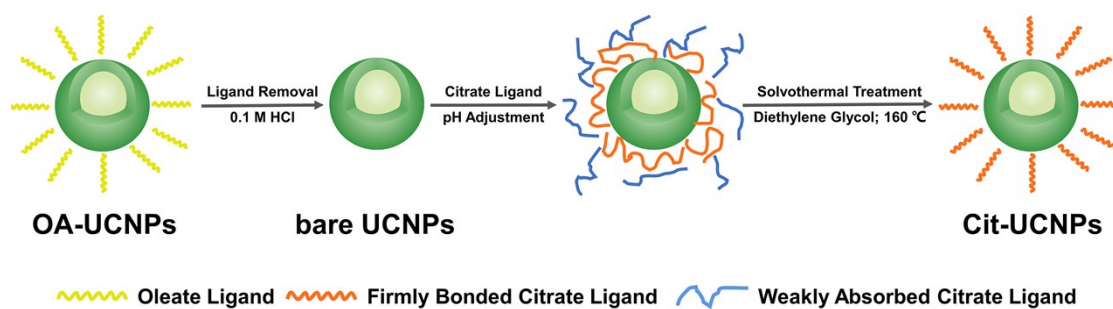


Figure S4. Schematic illustration of the experimental design for the surface modification of UCNPs with citrate ligand.

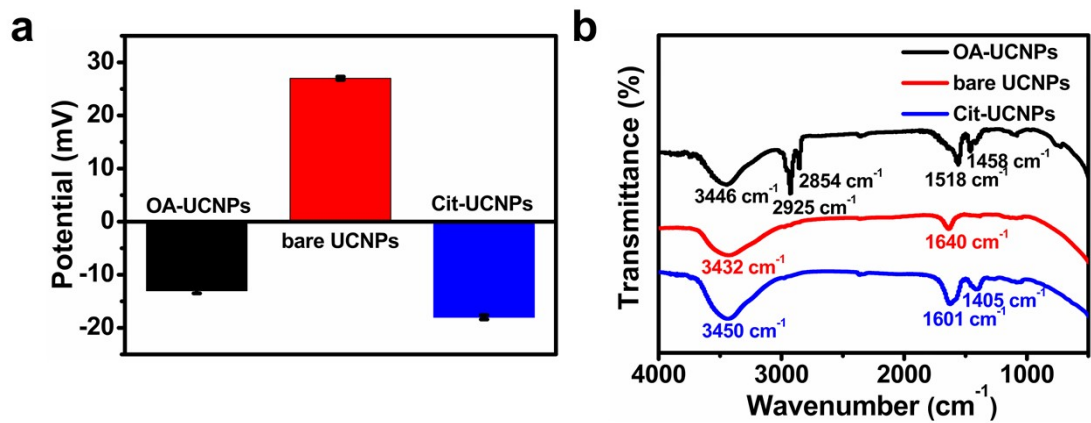


Figure S5. (a) Zeta potentials of OA-UCNPs, bare UCNPs, and Cit-UCNPs respectively. (b) FTIR spectra of OA-UCNPs, bare UCNPs, and Cit-UCNPs respectively.

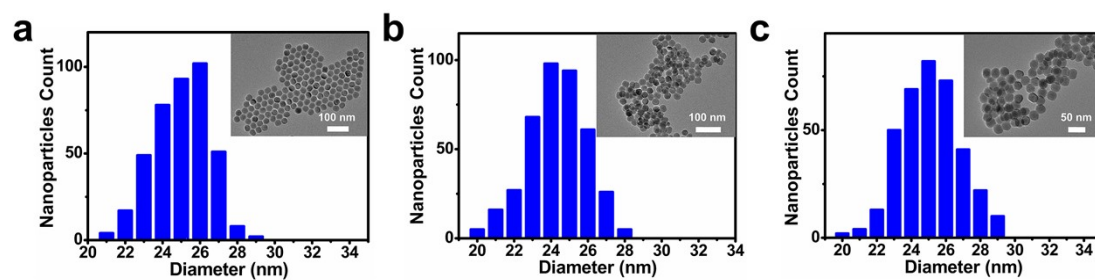


Figure S6. Histograms of particle size for UCNPs (the data was obtained from the TEM images over more than 400 UCNPs). Insets: TEM images of UCNPs. (a) OA-UCNPs. (b) Bare UCNPs. (c) Cit-UCNPs.

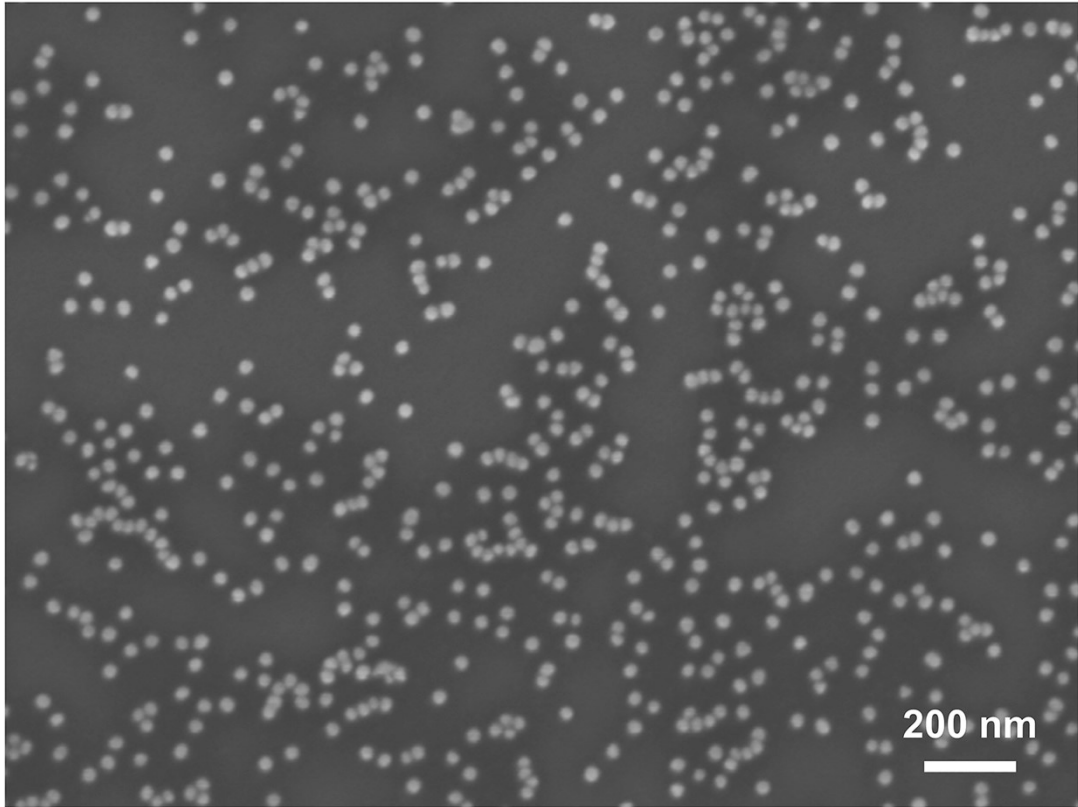


Figure S7. SEM image of AuNPs.

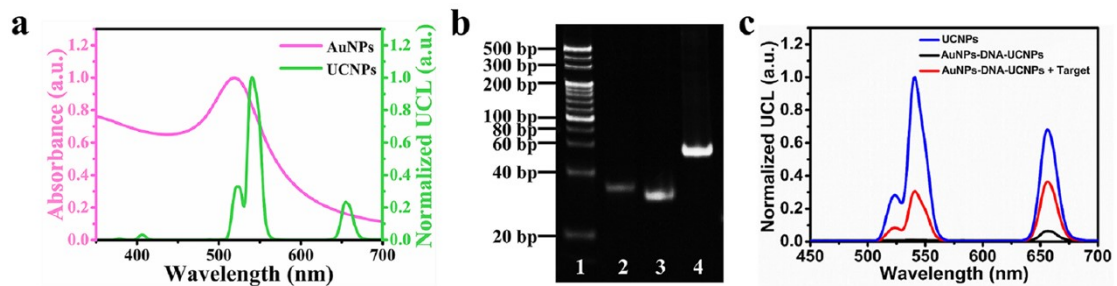


Figure S8. (a) The UCL spectrum of UCNPs and the UV-vis absorption spectrum of AuNPs. (b) Polyacrylamide gel electrophoresis (PAGE) of different samples. Lane 1, DNA marker; Lane 2, target; Lane 3, HP DNA; Lane 4, target + HP DNA. (c) The UCL spectra of different materials: UCNPs, AuNPs-DNA-UCNPs, and AuNPs-DNA-UCNPs incubated with $1\mu\text{M}$ target.



Figure S9. (a) The UV-vis absorption spectra of AuNPs + Freezing, AuNPs, and AuNPs-DNA + Freezing. (b) The images of AuNPs-DNA (left) and AuNPs (right) after addition of 1 M NaCl. (c) The images of AuNPs-DNA + Freezing (left) and AuNPs + Freezing (right) after addition of 1 M NaCl.

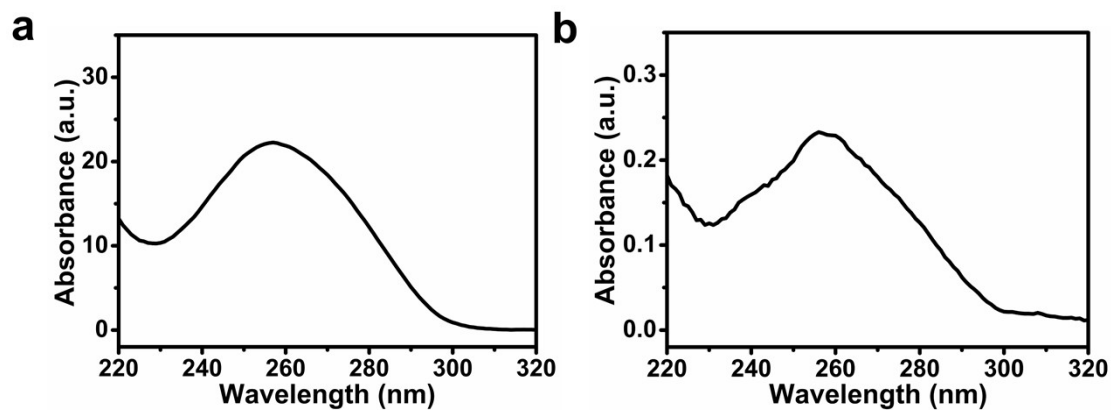


Figure S10. (a) Ultra-micro spectrophotometer spectrum of original HP DNA. (b) Ultra-micro spectrophotometer spectrum of HP DNA in the supernatant after the connection of AuNPs with HP DNA.

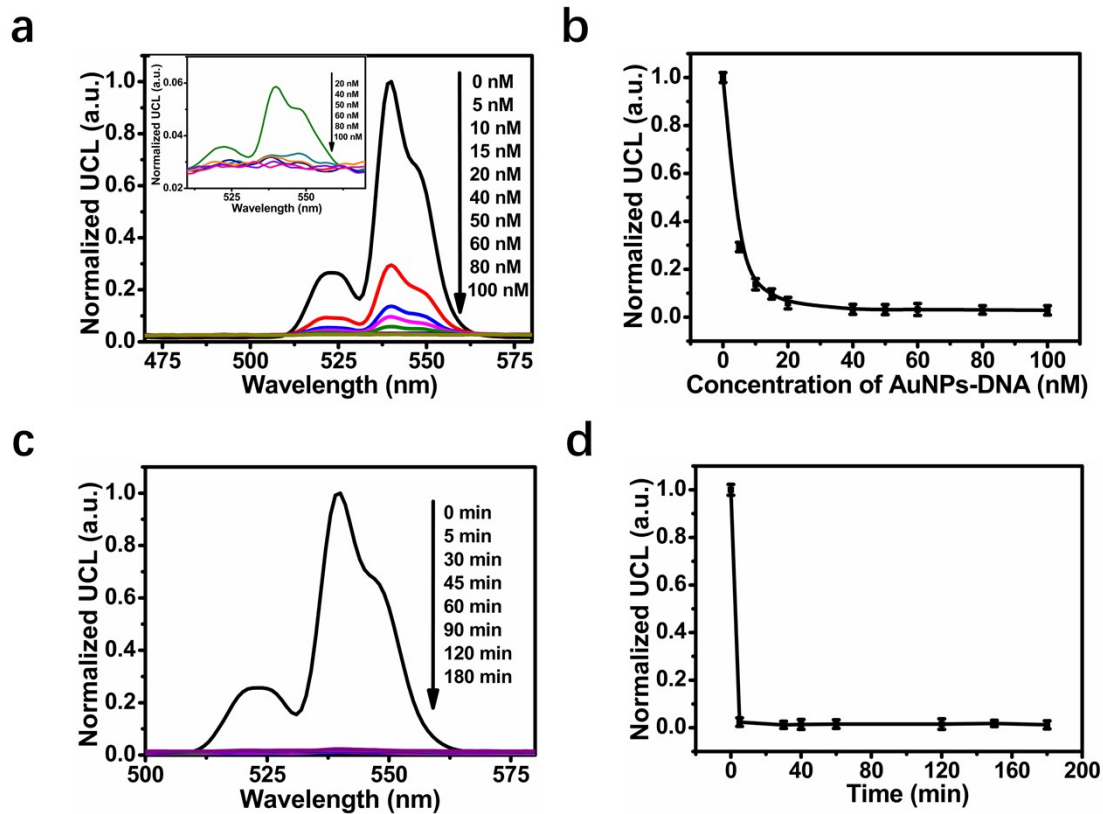


Figure S11. (a, b) Luminescence quenching with various concentrations of AuNPs-DNA. (c, d) Time dependence of the luminescence quenching degree with 1 mg/mL UCNPs and 20 nM AuNPs-DNA. Data are represented as mean values \pm SD ($n = 3$).

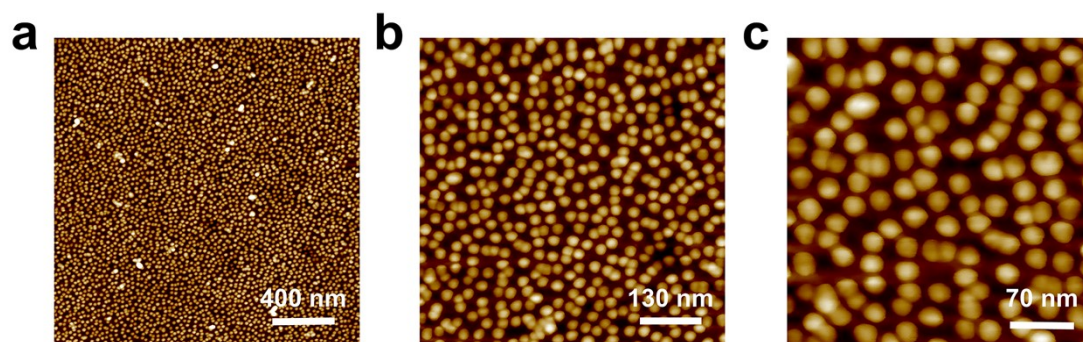


Figure S12. AFM images of immobilized AuNPs on the quartz glass plate.

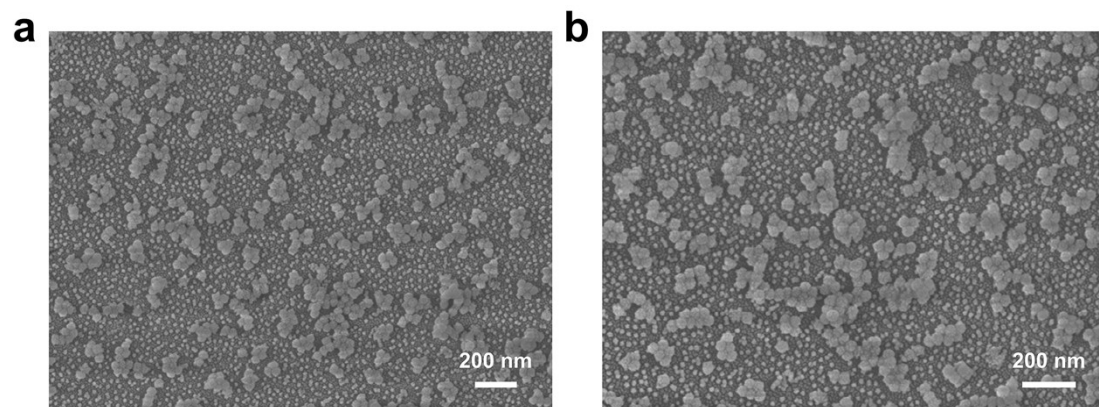


Figure S13. SEM images of AuNPs-DNA-UCNPs solid-phase biosensor.

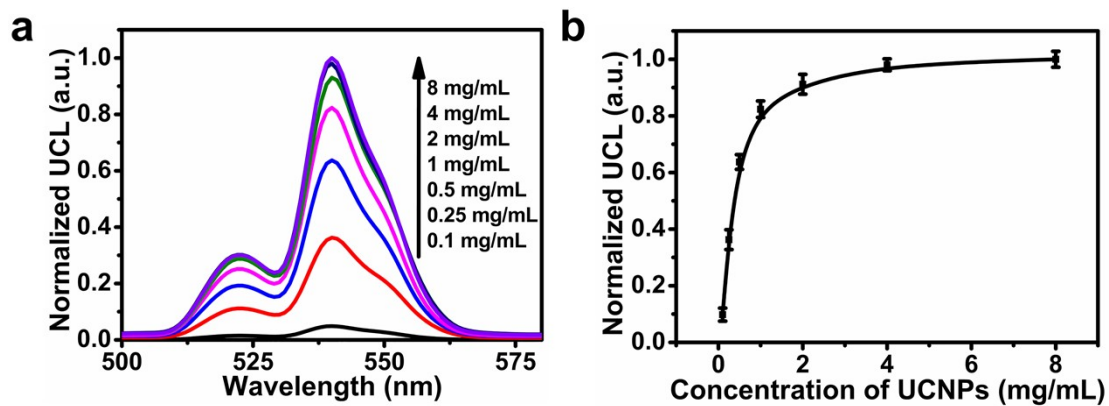


Figure S14. (a) UCL spectra against different concentrations of UCNP from 0.1 mg/mL to 8 mg/mL in the AuNPs-DNA-UCNP solid-phase biosensor. (b) The curve of the UCL with various concentrations of UCNP. Data are represented as mean values \pm SD ($n = 3$).

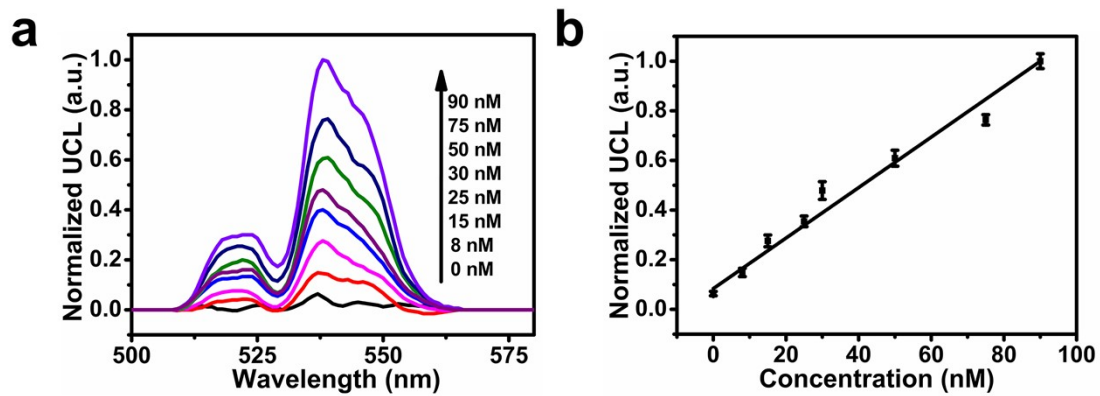


Figure S15. (a) Detection of virus-specific nucleic acid sequences in mouse serum by AuNPs-DNA-UCNPs solid-phase biosensor in the range of 8–90 nM. (b) Linear fitting curve of the UCL within the range of 8–90 nM target. Data are represented as mean values \pm SD ($n = 3$).

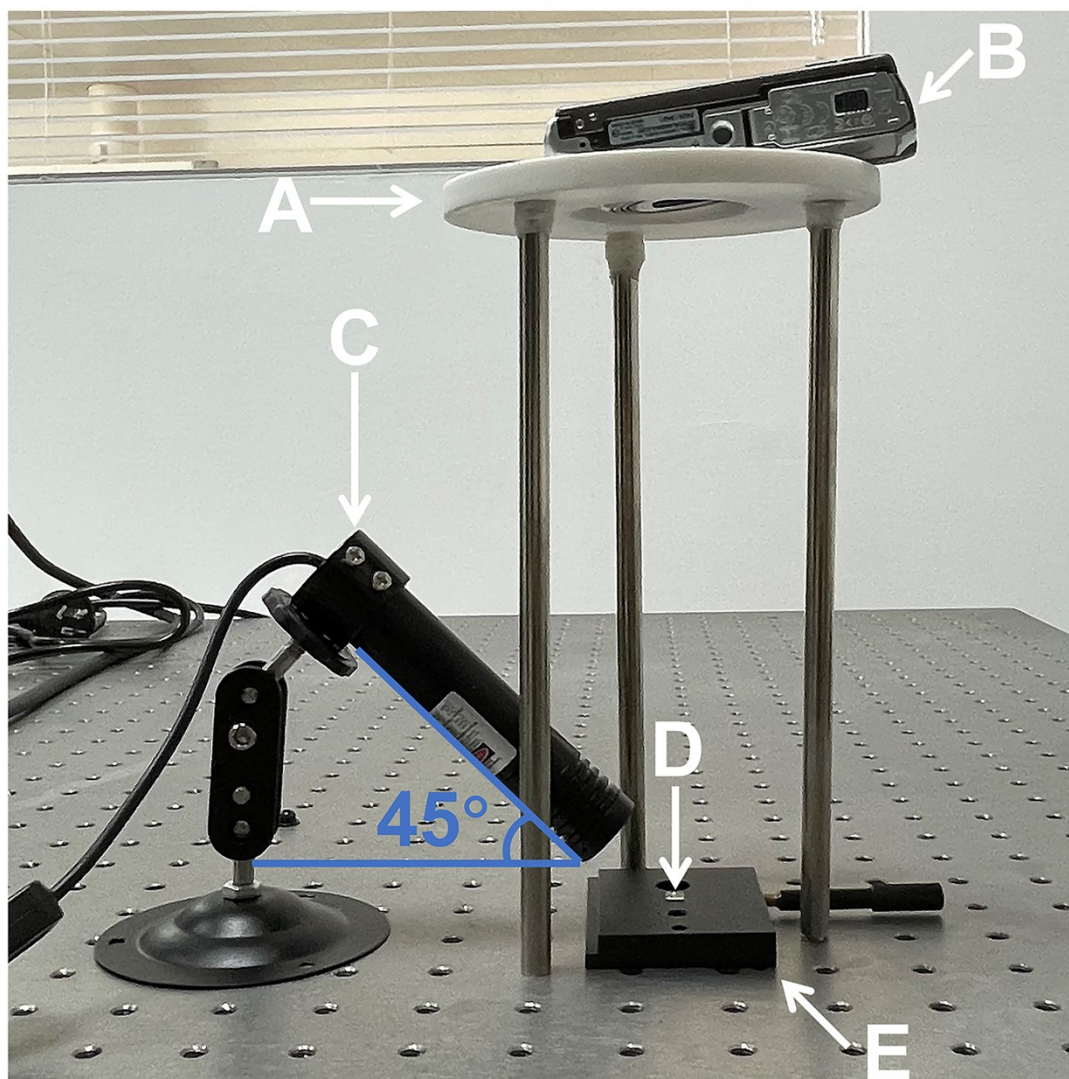


Figure S16. (a) The home-built luminescence image capture device. (A) Removable bracket; (B) Digital camera; (C) 980 nm laser; (D) Testing sample; (E) Sample stage.

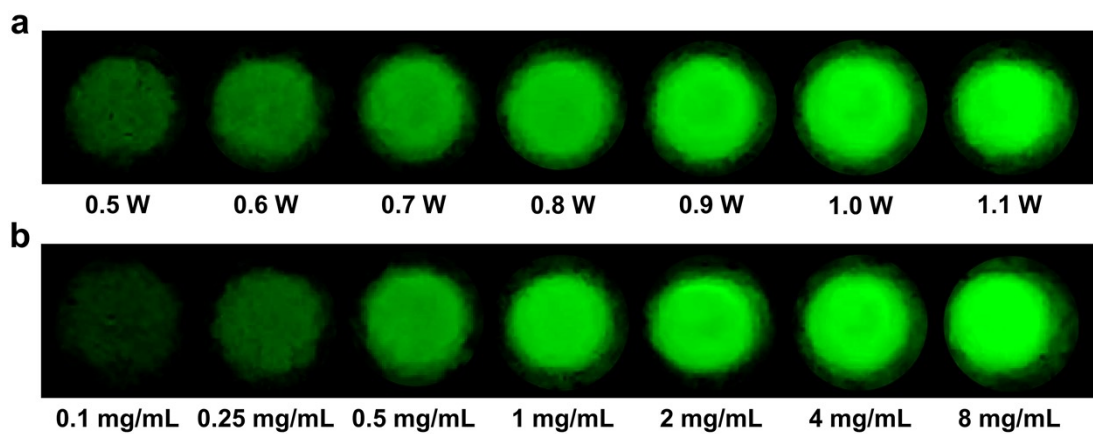


Figure S17. The light spot images of quartz glass plate under different conditions. (a) Different exciting powers from 0.5 W to 1.1 W. (b) Different concentrations of Cit-UCNPs from 0.1 mg/mL to 8 mg/mL.

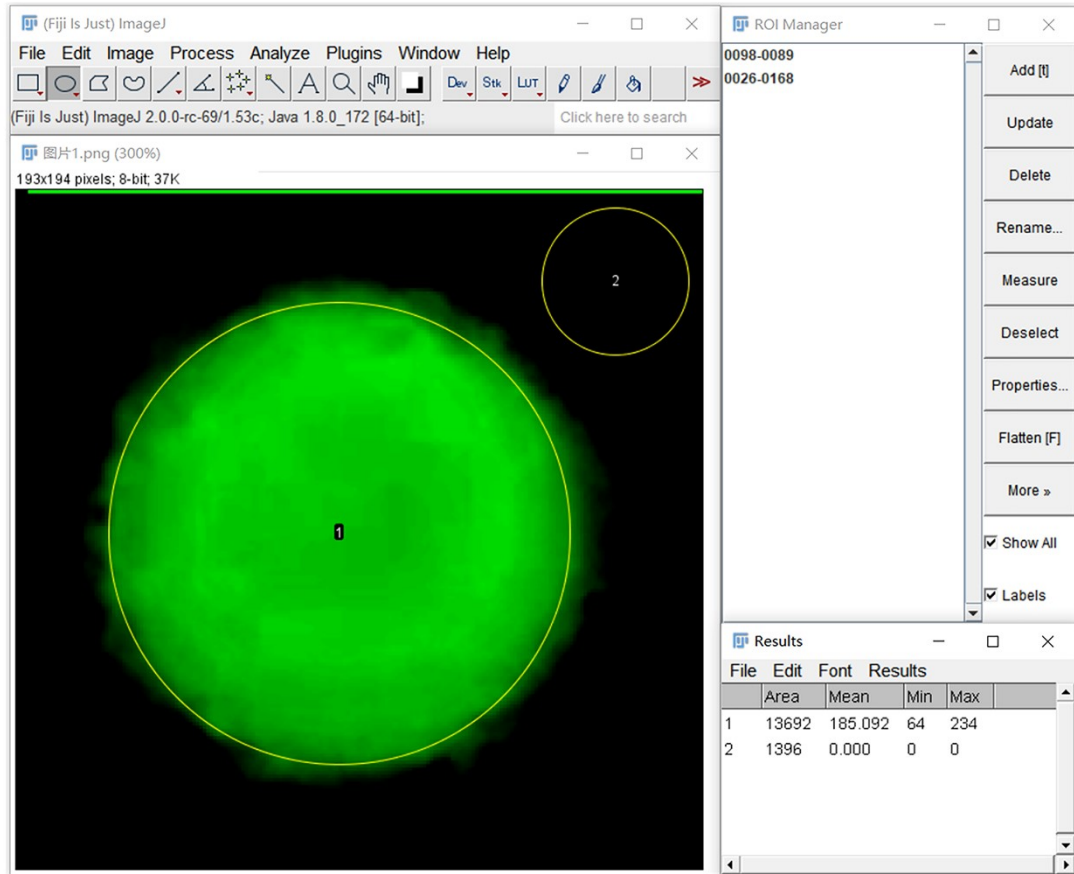


Figure S18. Image processing and analysis interface of ImageJ software.

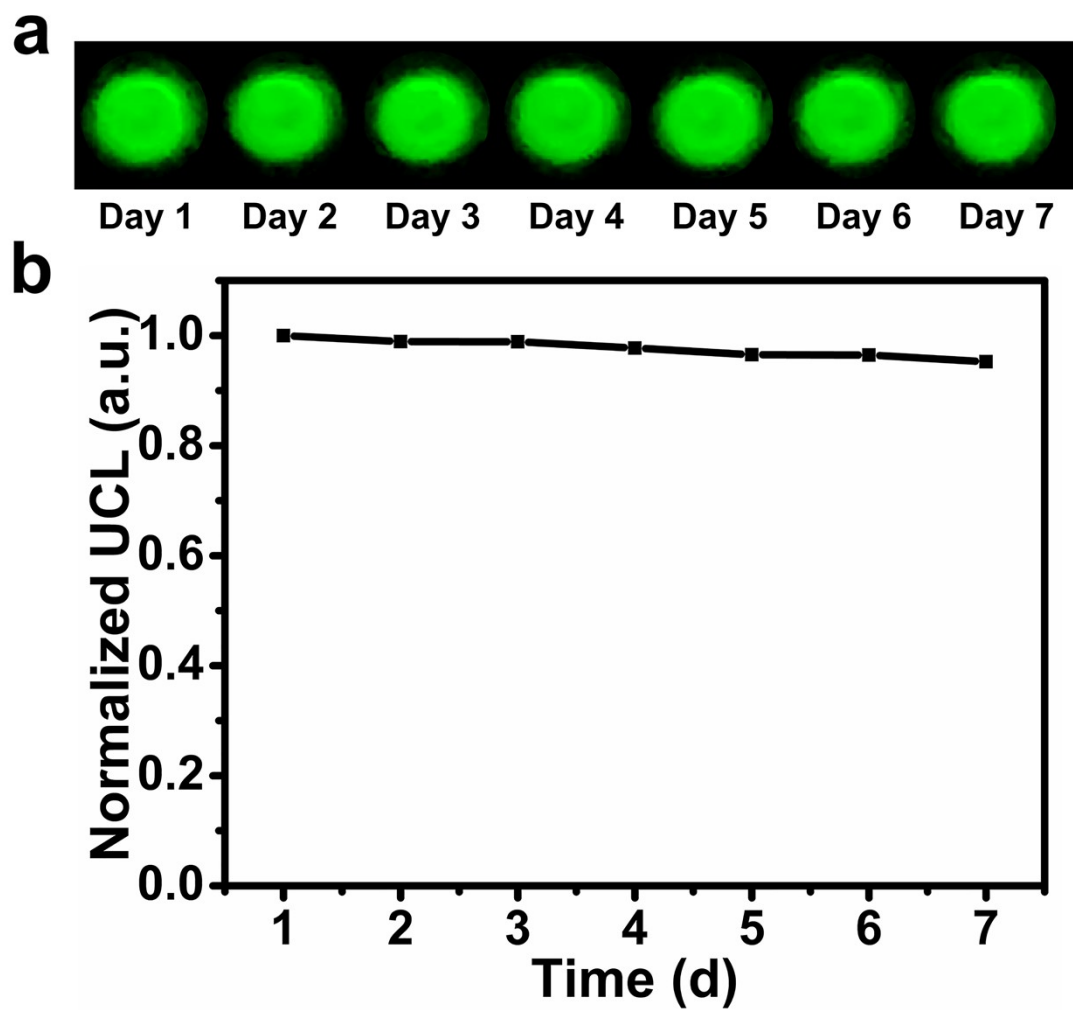


Figure S19. The luminescence stability of AuNPs-DNA-UCNPs solid-phase biosensor within a week.

Table S1. DNA sequences used in this study.

Name	Sequences (from 5' to 3')
	NH ₂ -
HP DNA	CCAGCGTGTACTTGTAACCGTCAAATGATCCGGGTCTGGTG GGAGCGAGTACACG-HS
Target	CGCTCCCACCAGACCCGGATCATTTTGACGGTTACAAGTACA CGCTGG
Mis-1	CGCTGCCACCAGACCCGGATCATTTTGACGGTTACAAGTACA CGCTGG
Mis-3	CGCTGCCACCAGTCCCGGATCATTTTGACGGTAACAAGTACA CGCTGG
Mis-5	CGCTGCCACCAGTCCCGGTTTATTAGACGGTAACAAGTACA CGCTGG
Mis-7	CGCTGCCACCAGTCCCGGTTTATTAGACGGTAACAAGAACA CCCTGG

Table S2. The mass of HP DNA in AuNPs-DNA probes.

	HP DNA concentration (ng/μL)	Volume (μL)	HP DNA mass (ng)
Original solution	725.10	2.50	1812.75
Supernatant fluid	7.53	100.00	753.32
AuNPs-DNA probes	—	—	1059.43

Table S3. EDS results for glass modification.

Element	Atomic Composition (%)	
	RCA	APTES
C	2	37
N	2	13
O	70	45
Si	27	5

Table S4. Recovery tests of virus-specific nucleic acid sequences in mouse serum samples.

Samples	Added (nM)	Measured \pm SD (nM)	Recovery (%)	RSD (n = 3, %)
1	10	9.52 \pm 0.21	95.2	2.2
2	20	21.72 \pm 1.21	108.6	5.6
3	40	40.92 \pm 1.50	102.3	3.7
4	60	63.54 \pm 2.84	105.9	4.5
5	80	77.76 \pm 5.55	97.2	7.1